Research Article

A novel tri-generation energy system integrating solar energy and industrial waste heat

Hamed POURFARZAD[1,*] , Mohammad SAREMIA[2] , Mohammad Reza GANJALI[1,3]

[1]Center of Excellence in Electrochemistry, Faculty of Chemistry, University of Tehran, Tehran, Iran
[2]Department of Electrical Engineering, College of Technical and Engineering, West Tehran Branch Islamic Azad University, Tehran, Iran
[3]Endocrinology & Metabolism Research Center, Tehran University of Medical Sciences, Tehran, Iran

ABSTRACT

Global warming has forced researchers to find an alternative for fossil fuels and to enhance the energy efficiency of processes in industries. Waste heat recovery has a significant potential to reduce fossil fuel consumption and energy performance enhancement. The study cycle is a tri-generation system, heating, electrical power, that can capture carbon dioxide gas. The system works with the solar energy and waste heat of the cement plant. In this study, a model for a completely new system has been developed based on renewable energies. Thermodynamic analysis for the energy system is performed, and the system is based on the organic Rankine cycle, absorption chiller, solar energy, and waste heat recovery from the exhaust gases of the cement plant stacks. The results of the analysis showed that the energy and exergy efficiencies were calculated to be 35.78% and 12.77%, respectively, and the total exergy destruction was calculated 277327 kW. Also, the optimisation result with the direct algorithm method with the objective function of exergy efficiency improved both efficiencies. In this optimisation, the exergy efficiency reached 16.39% and energy efficiency was calculated 49.04%. The optimisation with the objective function of total exergy destruction decreased the value to 216813 kW, which was significantly reduced from the base state of the system; while energy and exergy efficiencies were calculated to be 54.61% and 13.85%, respectively.

Cite this article as: Pourfarzad H, Saremia M, Reza M. Ganjali A novel tri-generation energy system integrating solar energy and indestrial waste heat. J Ther Eng 2021;7(5):1067–1078.

INTRODUCTION

Over the past century, the cement industry has experienced significant advances in various processes to increase efficiency and reduce pollutant emissions. Global cement production has reached about 2.8 billion tons per year and is expected to reach 4 billion tons annually. The cement industry has been by challenged many problems such as increasing energy costs, global warming, the need to reduce greenhouse gas emissions, and the supply of raw materials [1]. On the other hand, the cement industry has a high energy concentration in comparison to the other industrial and producing operations and 2% of the world energy consumption.

The cost of energy because of the need for a large amount of thermal energy for the various sectors of cement products, such as calibration, drying and furnace operation, and power for the electric fan, mill and conveyor [2, 3]. Studies express that about 50% of cement emissions occur during the conversion of limestone to calcium oxide. After the combustion of fuels, about 40% of the furnace gas emissions with the transport of about 5%, and electricity consumption in the production process is about 5% [4]. The effect of greenhouse gases on land heating was assessed by the earth heating potential unit which showed how much greenhouse gas caused global warming compared to the reference gas. For a 100-years interval, the potential for global warming of carbon dioxide gases, CH_4, and N_2O has been reported to be 1.25 and 298, respectively. Researches have indicated that carbon dioxide and methane concentrations have increased by 36% and 148% since 1750 [5]. The combustion of fossil fuels has accounted for about 75% of the increase in carbon dioxide emissions from human activities over the past 20 years. The main source of carbon dioxide emissions is the fossil fuel-based generation unit, accounting for about 32% of carbon dioxide emissions. Next, the largest source of carbon dioxide emissions is heating and cooling, which is about 33% of carbon dioxide emissions. About 65% of carbon dioxide emissions are associated with electricity generation and heating and cooling, both of which are directly related to human energy needs [5].

Distributed generation systems are used to optimize energy consumption, reduce losses due to transmission and distribution of electrical energy in the network, and reduce the pollution caused by the combustion of fossil fuels at large power plants [6]. Large-scale electric power generation and its transmission to consumers are a huge loss. On the other hand, large power plants have had low electrical efficiency due to production capacity. In addition, they have high costs for investment, installation, and commissioning as well as maintenance, and they increase the environmental pollutants. The set of these criteria and factors such as greater reliability, restructuring in the electricity industry led the countries of the world to the use of separate production processes [7]. Combined cooling, heating, and power generation cooling, along with new technologies is a way to solve global energy problems, including energy shortages, energy supply security, pollution control, and the energy economy.

Regarding the utilization of low-temperature sources, Organic Rankine Cycle (ORC) power systems have been proven to be one of the significant options. The organic working fluid in ORC power systems that has a lower boiling point than water grants this advantage. In an article, thermodynamic, economic, and environmental assessments were carried out for an ORC power system used for waste heat recovery [8]. Ahmed et al. [9] developed a design methodology for waste heat recovery using an ORC power system in cement plants. They claimed that the effectiveness of the ORC power system can be increased up to 95% by using R134a as a working fluid. Another study proposed an ORC power system for waste heat recovery of a cement factory in Sabzevar, Iran [10].

Al-Sulaiman et al. [11] analyzed and optimised thermo-economic for three different co-generation systems that used biomass, fuel cells, and solar panels, all of which are based on the ORC. They performed exergy modelling and economic analysis of the systems using the SPECO method. In this research, the application of thermo-economic analysis methods and optimisation of cogeneration systems have been investigated. Puig-Arnavat et al. [12], provided a model for design, optimisation, and simulation of a small-scale tri-generation system in Spain based on biomass gasification. They compared five different configurations, and all suggested configurations have a minimum efficiency of 27%, which is in line with the standard power generation in Spain. In a review study, Combined Cooling, Heating, and Power system (CCHP) was introduced as an instance of distributed generation systems to explore a variety of these systems. The history of the development of these systems has been analysed, and also the use of renewable energies, including wind and solar energy, is predicted to increase in the near future [13]. A small-scale tri-generation system based on fuel cells was developed by Wang et al. [14] to meet the needs of cooling, heating, and power of domestic applications. Another study proposed a micro-scale tri-generation system based on solar energy. They conducted their analysis based on two winter and summer modes. The results of the exergy analysis indicated that solar collectors and auxiliary boilers were two major sources of exergy destruction [15]. A hybrid ORC system driven by waste heat and solar energy was introduced by Bellos et al. [16] to maximise the electricity production of the system. In this study, several working fluids were examined. A thermo-economic assessment was performed for an ORC system that used solar energy, waste heat, and geothermal energy [17]. Moreover, particle swarm optimisation was performed to maximise heat recovery and net present value. Another integration of solar

flat plate and waste heat recovery was exploited for hydrogen production [18]. A solar-assisted Kalina cycle integrated with waste heat recovery was developed [19]. The waste heat was provided by flue gas of a 500 MW subcritical coal-fired power plant. They established that this configuration can prevent 1008 tons of CO_2 emissions annually. For waste heat recovery in the cement industry, Júnior et al. [20] proposed the Kalina cycle for a cement plant in Brazil that was proved to be a favourable option due to the cost value regarding the Brazilian tariff market. A solar/biomass-based-multigeneration system was proposed and analysed by Ghasemi et al [21]. Moreover, they performed multi-objective optimisation to obtain the minimum product cost rate and maximum performance of the system. Another study developed an optimal model to meet the needs of a cement plant [22]. The system can provide the heating, water, and power requirements of a cement plant. Moreover, thermoeconomic and environmental analyses were performed for the energy hub. Biogas-based cogeneration was developed by Chakyrova[23] to perform thermoeconomic analysis on it. The specific exergy cost method was exploited and several environmental conditions were taking into account. In another study, energy, exergy, economic and environmental analyses were performed on a refrigeration system [24]. Two single-optimisation methods were performed considering exergy and economic performance of the system. Ahmadi et al. [25] performed a thermodynamic and environment assessment on the Ericsson engine. They also conducted a revolutionary-based multi-objective optimisation on the system.

Integrating renewable energy with CO_2 capture has drawn interests among researchers. A novel solar-assisted post-combustion carbon capture system was proposed by Jordán et al. [26] in Mexico. Solar energy was exploited in this cogeneration system to mitigate the energy penalty imposed by the CO_2 capture process. An experimental study suggested using concentrated solar power for calcium looping that is one of post-combustion carbon capture technology [27]. Another study proposed the integration of solar energy and carbon capture and storage (CCS) systems to produce methanol [28]. Novotny et al. [29] compared waste heat recovery systems combined with different types of CCS combined including pre and post-combustion technologies. Another study was carried out by Jakobsen et al. [30] that different CCS system was compared for a cement plant in Norway. They performed a techno-economic analysis to investigate the impact of CCS on the cement production cost.

Hence, this article proposes a tri-generation energy system that takes The Abyek cement plant as a case study which is located in Qazvin, Iran. The goal of the energy system is to enhance the energy efficiency of the cement plant and to reduce the pollution of the exhaust gases from the stacks of the cement factory. And these can lead to energy consumption management of the cement plant finally.

Energy sources of the tri-generation energy system are solar energy and waste heat that is recovered from the flue gases of the cement plant. This energy system can produce power, hot water for residential purposes, and carbon dioxide. Another goal of the study is to low-temperature heat sources such as industrial heat loss and renewable energy sources. Energy and exergy analyses of the cycle are carried out and reported to evaluate the performance of the system in both energy and exergy views. Moreover, a single objective optimisation with the direct algorithm is performed for two objective functions such as exergy efficiency and exergy destruction separately.

MATERIAL AND METHOD

System Description

As presented in Figure 1, the exhaust gas from the stacks of the cement plant comes into the vapour generator and increases the heat of the organic working fluid that is considered to be R123 in this energy system. The absorption chiller cycle uses solar energy to cool down the carbon dioxide gas required to be extracted. The flue gas from the vapor generator enters cooler 2 to reach a temperature of about 50 °C to provide the absorption conditions. The mono-ethanol-amine (MEA) solvent is contacted to the cement plant flue gas in the absorber column. In the stripper column, the CO_2 is extracted from the CO_2 reach solution at high-temperature. The high-temperature of the stripper is provided by hot water. Finally, the MEA solvent is cooled and returned to the absorption column to continue the process as a closed cycle. The ABS2 and STP stand for absorber 2 and stripper, respectively. And HEX 2 denote heat exchanger 2.

MODELING

Energy Analysis of The Tre-Generation System

Based on the conservation law of mass, and the first and second laws of thermodynamics equation are yield for each component of the tri-generation energy system. Therefore, each component of the system and the overall system is taken as a control volume, and the mass, energy, and exergy balances are written for them.

Energy Analysis of The PV/T Subsystem

The rate of useful energy absorbed by the water in the panel is determined from the following equations [31]:

$$\dot{Q}_u = \dot{m} C_p \left(T_{out} - T_{in} \right) \tag{1}$$

$$\dot{Q}_u = A_p F_R \left[\left(\tau \alpha \right) 1 - Q_L \right] \tag{2}$$

$$F_R = \frac{\dot{m} C_p}{U_l A_p} \left[1 - e^{\left\{ \frac{F' U_l A_p}{\dot{m} C_p} \right\}} \right] \tag{3}$$

Figure 1. Schematic of a tri-generation system based on the solar and biomass energy.

$$\eta = \frac{\dot{Q}_u}{IA_p} \tag{4}$$

$$\dot{W} = \eta_p I \beta_p \tau_g A \tag{5}$$

In the equations above, AP is the panel area (m²), and η_{in} is the panel efficiency. The I represents the values of the instantaneous radiation reached the panel area (W/m²). The FR is the panel efficiency coefficient (W/m².K), and the $\dot{m}$ presents the inlet fluid mass flow to the panel (kg/s). Cp is the thermal capacity of the fluid used in the panel (kJ/kg.K). Tin and Tout are the fluid inlet and outlet temperature from the panel in °C, respectively.

The coefficient of Liu and Jordan correlation [32]:

$$r_d = \left(\frac{\pi}{24} \right) \frac{\cos(\omega) - \cos(\omega_{ss})}{\sin(\omega_{ss}) - \left(\frac{2\pi\omega_{ss}}{360} \right)\cos(\omega_{ss})} \tag{6}$$

In which rd is defined as the ratio of hourly radiation to the daily radiation. And ω_{ss} denotes the angle in the evening which can be obtain from equation No. 8. The coefficient of Collares Pereira and Rabl correlation [32]:

$$r = \frac{\pi}{24}(a + b\cos(\omega)) \frac{\cos(\omega) - \cos(\omega_{ss})}{\sin(\omega_{ss}) - (\frac{2\pi\omega_{ss}}{360})\cos(\omega_{ss})} \tag{7}$$

Here, r is defined as the ratio of total hourly radiation (I) to total daily radiation (H). In the equations above, the angle in the evening is in degrees, which is calculated from the following equation [32]:

$$\omega_{ss} = \arccos(-\tan(L)\tan(\delta)) \tag{8}$$

$$\delta = 23.45\sin\left[\frac{360}{365}(284+N)\right] \tag{9}$$

In which, N represents the number of days.

Energy Analysis of The ORC System

The conservation laws of mass and energy for a turbine are defined as follows:

$$\dot{W}_{Turb} = \dot{m}_5 h_5 - \dot{m}_6 h_6 \tag{10}$$

The thermodynamic process in the adiabatic turbine is assumed. The turbine isentropic efficiency is expressed as follows:

$$\eta_{is,Turb} = \frac{\dot{W}_{Turb}}{\dot{W}_{is,Turb}} \tag{11}$$

The heater supplies the required heating load with the turbine outlet flow, assuming no pressure loss occurs and the outlet flow is saturated vapour. The mass and energy balances equations in the heater are as follows:

$$\dot{m}_{12} = \dot{m}_{11} \tag{12}$$

$$\dot{Q}_{HL} = \dot{m}_{11}(h_{12} - h_{11}) \tag{13}$$

In which, QHL is the heating load (kW).

Assuming that the pumping process is adiabatic, the thermodynamic equations governing pump 2 are as below:

$$\dot{m}_7 = \dot{m}_8 \tag{14}$$

$$\dot{W}_{P2} = \dot{m}_7 v_7 (P_8 - P_7)\big/\eta_{is,p_2} \tag{15}$$

Here, the v presents a specific volume of fluid (m³/kg), and η_{is,p_2} is isentropic efficiency of the pump.

The equations for the pump 1, pump 3 and pump 4 are similar. Assuming that the pressure remains stable in the process of receiving the heat in the economizer and evaporator, the laws of conservation of mass and energy governing them are as described below.

$$\dot{m}_1 = \dot{m}_2 \tag{16}$$

$$\dot{m}_5 = \dot{m}_8 \tag{17}$$

$$\dot{m}_5(h_5 - h_8) = \dot{m}_1(h_1 - h_2) \tag{18}$$

The electric generator outlet is defined as the ratio of the electrical power outlet to mechanical power:

$$\eta_{gen} = \frac{\dot{W}_{elec}}{\dot{W}_{net}} \tag{19}$$

Electric power is obtained from the difference in turbine power and total consumption power of the pump. Also, the electric power is a function of the electric generator's efficiency:

$$\dot{W}_{elec} = (\dot{W}_{Turb} - \dot{W}_{p2}) \times \eta_{gen} \tag{20}$$

Energy Analysis of The Absorption Chiller Subsystem

The cooling load of the cycle is provided by an evapourator, a component of the absorption chiller subsystem, and the equation is as follows:

$$Q_{CL} = \dot{m}_{39}(h_{39} - h_{40}) \tag{21}$$

Energy Analysis of Subsystem CCS

The amount of heat exchanged in the stripper, cooler and absorber are as follows:

$$Q_{STP} = \dot{m}_{25}C_p(T_{25} - T_{26}) \tag{22}$$

$$Q_{Cooler1} = \dot{m}_{22}(h_{23} - h_{22}) \tag{23}$$

$$Q_{ABS2} = \dot{m}_{39}C_p(T_{39} - T_{40}) \tag{24}$$

Exergy Analysis of Tri-Generation System

Exergy is a property that defines the capability of producing the useful work of a system with a certain amount of energy in a given state. In exergy analysis, the first state of the system is given, the maximum amount of useful work can be obtained when the process is reversible and the final state is a dead state. The dead state defines as the temperature and pressure of the environment, kinetic and potential energy has considered negligible. The exergy of the system in the dead state equal to zero. Since exergy depends on the final state of the system, it can be expressed that exergy is the combined property of the system and the environment [33].

Exergy is transmitted in three ways: by work, by heat transfer, and by mass transfer to the control volume. The exergy balance can be written in different states of the system, in control volumes, and in the steady or dynamic states. Regarding the fact that most of the components used in this study are considered as control volume, the exergy balance for a control volume is given below [34]:

$$0 = \sum_j \left(1 - \frac{T_0}{T_j}\right)\dot{Q}_j - \dot{W}_{cv} + \sum_i \dot{m}_i x_i - \sum_o \dot{m}_o x_o - \dot{X}_D \tag{25}$$

In the equation above, $\dot{Q}_J$ represents the heat transfer rate from the control volume boundary at its temperature that is presented by T_J, $\dot{W}_{CV}$ is work generated by the control volume. X_0 and X_1 are the specific exergies for inlet and outlet flows of the control volume (kJ/kg). $\dot{X}_D$ defines the exergy destruction in kW, which is a result of irreversibility within the control volume and is obtained from the following equation [34]:

$$\dot{X}_D = T_0 \dot{S}_{gen} \tag{26}$$

In which T_0 is the dead state temperature (K), and $\dot{S}_{gen}$ represents the entropy rate in kJ/Ks.

The x_0 and x_1 values can include four types of exergy: physical exergy, chemical exergy, kinetic exergy, and potential exergy as follows [34]:

$$x = x_{PH} + x_{CH} + x_{KN} + x_{PT} \tag{27}$$

Since this study, the velocity and height of flows are considered negligible, and it is assumed that these flows are unlikely to have a chemical reaction with the environment. As a result, the specific exergy of flow is transferred only by physical exergy and is written as follows:

$$x = x_{PH} = (h - h_0) - T_0(s - s_0) \tag{28}$$

In which, the index 0 is related to the dead state. And h represents specific enthalpy (kj/kg), and the S is the specific entropy (kj/kg.K)

Exergy Analysis of Subsystem PV/T

The PV/T subsystem is considered as a control volume, the exergy balance for it can be expressed as follows:

$$\dot{X}_s - (\dot{m}_{14}x_{14} - \dot{m}_{13}x_{13}) - \dot{X}_{D,panel} = 0 \tag{29}$$

In the equation above $\dot{X}_S$ is the inlet exergy to the collector from the sun (kW), by considering the sun as a black body it can be expressed as below [35, 36]:

$$\dot{X}_s = I.A_p\left(1 + \frac{1}{3}\left(\frac{T_0}{T_s}\right)^4 - \frac{4}{3}\left(\frac{T_0}{T_s}\right)\right) \tag{30}$$

In which T_s is the surface temperature of the sun assumed to be 6,000 Kelvin [31].

$$\dot{X}_{f-pump5} = \dot{W}_{P5} \tag{31}$$

$$\dot{X}_{p-ejec} = \dot{m}_{15}\left(x_{13} - x_{15}\right) \tag{32}$$

ORC Subsystem Exergy Analysis

The ORC subsystem consists of components, all of which are considered as the control volume. There is not

Table 1. Exergy balance equations for system components

Component	Fuel	Product
Turbine	$\dot{m}_5x_5 - \dot{m}_6x_6$	$\dot{W}_{Turb}$
Heater	$\dot{m}_6x_6 - \dot{m}_7x_7$	$\dot{m}_{26}x_{26} - \dot{m}_{25}x_{25}$
Vapour generator	$\dot{m}_1x_1 - \dot{m}_2x_2$	$\dot{m}_5x_5 - \dot{m}_8x_8$
Pump 2	$\dot{W}_{p2}$	$\dot{m}_8x_8 - \dot{m}_7x_7$

any heat dissipation from these components, therefore, the exergy loss is negligible. The exergy balance equations for each component of the tri-generation energy system are presented in Table 1.

Absorption Chiller Subsystem Exergy Analysis

The fuel and product exergy for this component is considered as follows considering the fact that the cooling load is provided by the evapourator in the absorption chiller subsystem:

$$\dot{X}_f = (\dot{m}_{14}x_{14} - \dot{m}_{15}x_{15}) \tag{33}$$

$$\dot{X}_p = \dot{m}_{40}(h_{39} - h_{40})\left(1 - \frac{T_0}{T_{39}}\right) \tag{34}$$

CCS Subsystem Exergy Analysis

Fuel and product exergy for the components of the CCS subsystem are as follows:

System Performance Evaluation

In evaluating the performance of a system, a suitable criterion should be chosen, and the performance of the system would be measured accordingly. In the assessment of energy systems, the efficiency of the first law, which is defined as the useful tool that is power generated by the system to the overall input power to the system, is considered as one of the system evaluation criteria. The efficiency of the first law is expressed as follows:

$$\eta_{total} = \frac{W_{Solar} + W_{Turb} + Q_{Heating} + \dot{m}_{CO_2}h_{CO_2}}{Q_{solar} + \dot{m}_{cement}h_{cement}} \tag{35}$$

Given that the first law of thermodynamics deals only with the quantity of energy and its conservation, we need another means to examine the quality of energy and analyse it during the process and generation of entropy. This criterion, called the efficiency of the second law of thermodynamics, is defined as the ratio of the performance of a

system to its function in a reversible state. The efficiency of the second law of thermodynamics for the whole system is as follows:

$$\psi_{total} = \frac{\dot{Ex}_{W,PV/T} + \dot{Ex}_{W,turb} + \dot{Ex}_{CO_2}}{\dot{Ex}_{solar} + \dot{Ex}_{Cement\_plant}} \quad (36)$$

RESULTS AND DISCUSSION

The analysis of the tri-generation system from the first law and second law (exergy) perspectives requires information such as system schematics and system design parameters (Table 3). The modeling is performed in the Engineering Equation Solver (EES) software [37]. The above-mentioned equations are applied, and the thermodynamic performance of the whole system, including thermal

Table 2. Exergy Balance equations for CCS System Components

Component	Fuel	Product
Stripper	$\dot{m}_{19}x_{19} - \dot{m}_{20}x_{20} + \dot{m}_{25}$ $(x_{25} - x_{26})$	$\dot{m}_{24}x_{24}$
Pump 3	$\dot{W}_{p3}$	$\dot{m}_{21}x_{21} - \dot{m}_{20}x_{20}$
Heat exchanger	$M_{47}x_{47} - m_{48}x_{48}$	$\dot{m}_{19}x_{19} - \dot{m}_{18}x_{18}$
Pump 4	$\dot{W}_{P4}$	$\dot{m}_{44}x_{44} - \dot{m}_{43}x_{43}$
Cooler 1	−	$\dot{m}_{23}x_{23} - \dot{m}_{22}x_{22}$
Cooler 2	$\dot{m}_{39}x_{39} - \dot{m}_{40}x_{40}$	$\dot{m}_3x_3 - \dot{m}_2x_2$
Absorber	$\dot{m}_{23}x_{23} - \dot{m}_{17}x_{17}$	$\dot{m}_4x_4 - \dot{m}_3x_3$

Table 3. System Design Parameters

Dead state temperature (°C)	15
Dead state pressure (kPa)	101.3
Turbine inlet pressure (kPa)	1760
Turbine inlet temperature (°C)	160
Isentropic turbine efficiency (%)	0.85
Evaporator1 temperature difference (°C)	10
Isentropic pumps efficiency (%)	0.7
Electric generator efficiency (%)	0.95
Exhaust gas flow rate (kg/s)	867
Exhaust gas temperature from the chimney (°C)	170
Turbine pressure ratio	2.5

Table 4. Thermodynamic performance of the system

Panel surface (m²)	221814
Generation heat (kW)	48.58
Power generation (kW)	16.29
Energy efficiency (%)	35.78
Exergy efficiency (%)	12.77

efficiency, exergy efficiency, required panel surface, generated power, and heat are presented in Table 4.

Exergy Destruction of System Components

In this section, the exergy destruction and the ratio of exergy destruction of each component to the total exergy destruction of each component, and the results are presented in Table 5. As presented in the table below, CCS, solar panel, and chiller are the largest sources of exergy destruction. While other components have less contribution to the overall exergy destruction.

In the CCS system, the most destruction occurs in the absorber and stripper towers due to the high-temperature difference between the inlet flow, the temperature of absorption and extraction. In the absorption tower, the difference in the temperature of the inlet gas and the absorption, temperature is the cause of the destruction. And in the stripper tower, the temperature difference between the flow containing CO_2 and MEA and the outlet flow is the reason. The available solutions to reduce this destructions are the use of adsorbents with a high absorption rates and low exhalation temperatures. Thus, in the heat exchangers and chiller evapourators, due to the high-temperature difference between the inflow and the flows, the amount of exergy destruction is significant.

Thermodynamic Sensitivity Analyses

Turbine Inlet Pressure Effect on Cycle Efficiency

Figure 2, shows the effect of turbine inlet pressure on energy and exergy efficiencies of the system. As shown in Figure 2, it decreases with increasing energy efficiency, and this decrease is due to an increase in the input energy of pump 2. Exergy efficiency is initially increased and then decreased, the increase is because of increasing the outlet exergy of the system in comparison to the inlet exergy. And, similarly, in the reduction trend, it is justified that the inlet exergy of the system has increased.

Effect of Turbine Inlet Temperature on Cycle Efficiency

Figure 3 illustrates the effect of turbine inlet temperature on energy and exergy efficiencies of the energy system. As shown in Figure 3, the energy efficiency decreases with increasing temperature from 80 to 180 °C. And this decrement is because of higher energy input than energy output.

However, for the exergy efficiency of the turbine input temperature, the outlet exergy of the system increases in terms of power or heat, which overcomes the increase of exergy inputs.

Effect of Fluid Mass Flow Rate in The Solar Cycle on Cycle Efficiency

Figure 4 demonstrates the effect of the mass flow rate of the fluid in the solar subsystem on the energy and exergy efficiencies of the whole cycle. As shown in Figure 4, the energy efficiency decreases with increasing mass flow rate in the solar cycle which points out that increasing the mass flow rate of the fluid in the solar cycle has been reduced the number of system products compared to the energy input of the system. The exergy efficiency has the same behaviour and is justified in the same way.

The Effect of Temperature of Exhaust Gases from The Cement Plant on The Cycle Efficiency

Figure 5 shows the effect of the temperature of the exhaust gases from the cement plant on the energy and exergy efficiencies of the proposed system. As illustrated in Figure 5, the energy efficiency increases with increasing mass flow rate of the fluid in the solar cycle which points out the fact that this rise in temperature has led to a drastic rise in the system's products compared to the input energy of the system. The exergy efficiency trend is similar to the energy efficiency trend and is justified similarly. The effect of this parameter on the overall efficiency of the system is very high, which reminds us of the effect of the amount of sunlight, which is one of the energy sources in this cycle.

Optimisation

In this section, single-objective optimisation is performed and the exergy efficiency of the system and the exergy destruction of the system components are separately considered as objective functions. The objective functions are maximising exergy efficiency and minimising exergy destruction. Six independent variables are selected by sensitivity analyses to optimise the performance. The variables are such as the ambient temperature, the temperature of cement plant flue gas, turbine input temperature, turbine

Table 5. Excessive Features of System Components

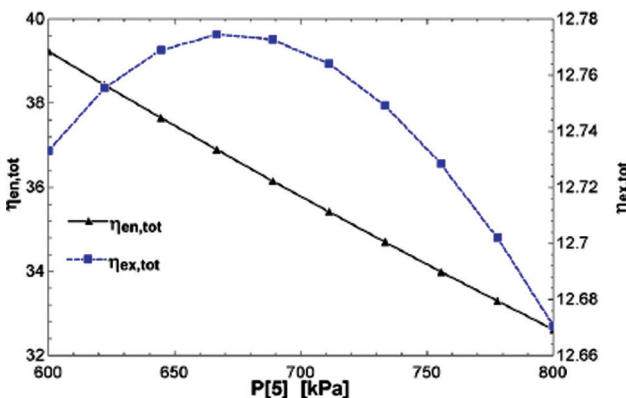| Components	$X_D(kW)$	$\overset{*}{Y}_D(\%)$
Solar Panel	120339	0.4341
Turbine	511.2	0.0018
heater	2326	0.008
Steam generator	47256	0.1704
Electrical generator	358.6	0.001
Pump 1	403.9	0.0014
Pump 5	303.4	0.00011
Absorption chiller	62619	0.2258
CCS	43150	0.1556
Total	277327	-

Figure 3. Effect of turbine input temperature on energy and exergy efficiencie.
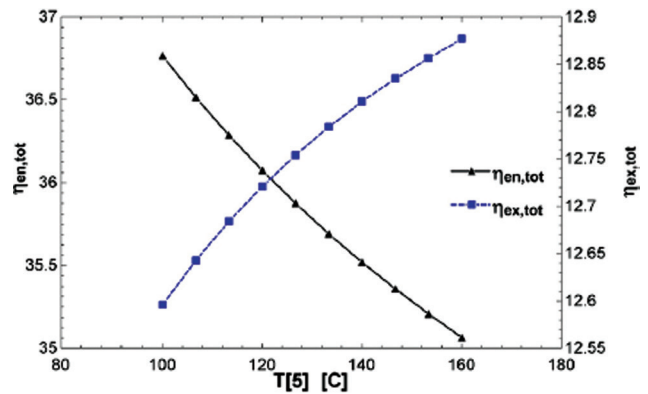
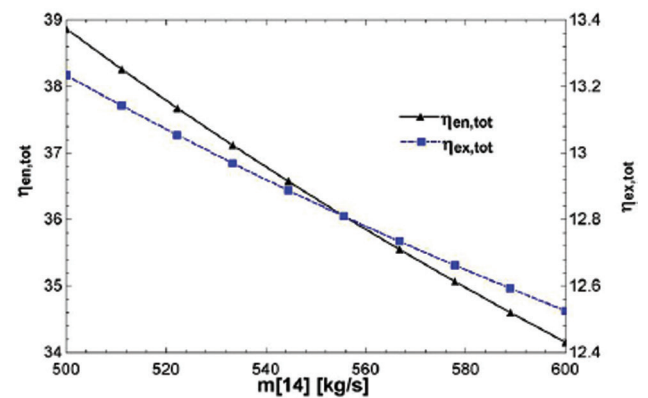**Figure 2.** Effect of turbine inlet pressure on energy and exergy efficiencies.

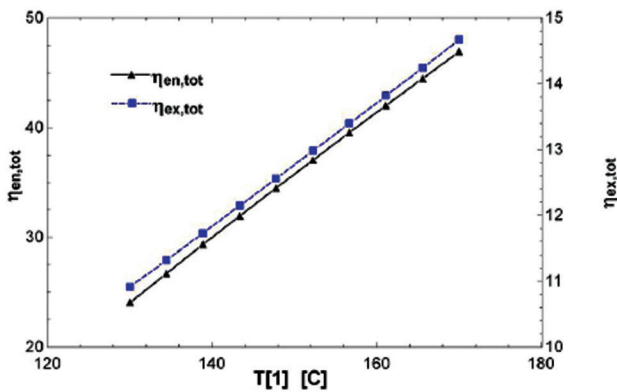**Figure 4.** Effect of the solar subsystem mass flow rate on energy and exergy efficiencies.

Figure 5. Effect of the exhaust gases temperature on energy and exergy efficienciesexergy efficiencie.

Table 6. Basic and optimal state values of decision variables for exergy efficiency objective function

	Base State	Optimum
Ambient temperature T[0] (°C)	25	23
The cement plant flue gas T[1] (°C)	150	169.8
Turbine inlet temperature T[5] (°C)	130	101.1
Turbine inlet pressure P[5] (kPa)	700	796
The flow rate of solar cycle working fluid $\dot{m}$	561.1	501.59
Heater temperature difference $\Delta \dot{T}_{Heater}$ (°C)	30	10.37
Objective function: exergy efficiency (%)	12.77	16.39
Energy efficiency (%)	35.78	49.04
Total exergy destruction	277327	223735

Table 7. Basic and optimal state values of decision variables for exergy destruction objective function

	Base state	Optimum
Ambient temperature T[0] (°C)	25	38.33
The cement plant flue gas T[1] (°C)	150	163.3
Turbine inlet temperature T[5] (°C)	130	110
Turbine inlet pressure P[5] (kPa)	700	700
The flow rate of solar cycle working fluid $\dot{m}$	561.1	516.7
Heater temperature difference $\Delta \dot{T}_{Heater}$ (°C)	30	20
Exergy efficiency (%)	12.77	13.85
Energy efficiency (%)	35.78	54.61
Objective function: Total exergy destruction (kW)	277327	216760

input pressure, the flow rate of solar subsystem working fluid, and temperature difference of the heater. The optimisation results for each objective function are presented in Tables 6 and 7.

CONCLUSION

In this study, a model for a completely novel system has been developed based on renewable energies. Thermodynamic analysis and single objective optimization are performed for a tri-generation system that produces power, heating and extracts carbon dioxide from flue gases of the cement plant in Qazvin, Iran. The results of all sections are as follows:

- The energy and exergy efficiencies were calculated to be 35.78% and 12.77%, respectively, and the total exergy destruction was calculated 277327 kW.
- From the exergy destruction of each component it was concluded that the solar panels, CCS, and absorption chiller destroy most of the exergy entering the system, and are considered to be the largest source of exergy destruction.
- In the sensitivity analysis, the energy efficiency remained constant with increasing the temperature difference, and the exergy efficiency decreased. The increase in the mass flow rate of working fluid in the solar subsystem reduced the energy efficiency and exergy of the cycle, and the increase in radiation was accompanied by increasing the efficiencies. Increasing the turbine inlet pressure reduced the energy efficiency and the exergy efficiency was increased. And the increasing the flow temperature to the turbine also reduced the energy efficiency. Changes in ambient temperature significantly increased the energy efficiency of the cycle. The energy and exergy efficiencies increased significantly with increasing the temperature of the exhaust gas from the cement plant.
- The result of optimisation using the direct algorithm in EES software with the objective function of exergy efficiency yielded a great deal in this efficiency so that the exergy efficiency reached 16.39% and the energy efficiency was calculated to be 49.04%. The optimisation with the total exergy destruction objective function reduced this value to 216813kW, which differs greatly from the base state of the system, while the energy and exergy efficiencies are calculated to be 54.61% and 13.85%, respectively.

NOMENCLATURE

0	Dead state condition
Ap	Panel Area
x	Total specific exergy

x_{chi}	Component specific chemical exergy
$\dot{X}_D$	Exergy destruction rate
η_{in}	Panel efficiency
I	Instantaneous radiation reached to the panel area
H	Total daily radiation
FR	Panel efficiency coefficient
$\dot{m}$	Fluid mass flow rate
N	Number of days
Cp	Thermal capacity
r	The coefficient of Collares Pereira and Rabl correlation
rd	The coefficient of Liu and Jordan correlation
v	The specific volume of fluid
$\dot{w}$	Work transfer rate
$\dot{Q}$	Heat transfer rate
$\dot{S}$	Entropy rate
$\overset{*}{\dot{y}}_D$	The ratio of exergy destruction of each component

Greek symbol

ω_{ss}	The angle in the evening
δ	Deflection angle
η	Energy efficiency
ψ	Exergy efficiency

Subscripts

ABS	Absorber
CH	Chemical
CL	Cooling
Cement	Cement plant
f	Fuel
Gen	Generator
HL	Heating load
In	Input
Is	Isentropic
KN	Kinetic
Out	Output
P	Pump
p	Product
PH	Physical
PT	Potential
S	Solar
STP	Stripper
Turb	Turbine

DATA AVAILABILITY STATEMENT

No new data were created in this study. The published publication includes all graphics collected or developed during the study.

CONFLICT OF INTEREST

The author declared no potential conflicts of interest with respect to the research, authorship, and/or publication of this article.

ETHICS

There are no ethical issues with the publication of this manuscript.

REFRENCES

[1] Schneider M, Romer M, Tschudin M, Bolio H. Sustainable cement production-present and future. Cem Concr Res 2011;41:642–50. https://doi.org/10.1016/j.cemconres.2011.03.019.

[2] Khurana S, Banerjee R, Gaitonde U. Energy balance and cogeneration for a cement plant. Appl Therm Eng 2002;22:485–94. https://doi.org/10.1016/S1359-4311(01)00128-4.

[3] Önüt S, Soner S. Analysis of energy use and efficiency in Turkish manufacturing sector SMEs. Energy Convers Manag 2007;48:384–94. https://doi.org/10.1016/j.enconman.2006.07.009.

[4] Mahasenan N, Dahowski RT, Davidson CL. The role of carbon dioxide capture and storage in reducing emissions from cement plants in North America. Greenh. Gas Control Technol., 2005, p. 901–9. https://doi.org/10.1016/B978-008044704-9/50091-4.

[5] Wu DW, Wang RZ. Combined cooling, heating and power: A review. Prog Energy Combust Sci 2006;32:459–95. https://doi.org/10.1016/j.pecs.2006.02.001.

[6] Singh B, Sharma J. A review on distributed generation planning. Renew Sustain Energy Rev 2017;76:529–44. https://doi.org/10.1016/j.rser.2017.03.034.

[7] Dincer I, Zamfirescu C. Renewable-energy-based multigeneration systems. Int J Energy Res 2012;36:1403–15. https://doi.org/10.1002/er.2882.

[8] Yi Z, Luo X, Yang Z, Wang C, Chen J, Chen Y, et al. Thermo-economic-environmental optimization of a liquid separation condensation-based organic Rankine cycle driven by waste heat. J Clean Prod 2018;184:198–210. https://doi.org/10.1016/j.jclepro.2018.01.095.

[9] Ahmed A, Esmaeil KK, Irfan MA, Al-Mufadi FA. Design methodology of organic Rankine cycle for waste heat recovery in cement plants. Appl Therm Eng 2018;129:421–30. https://doi.org/10.1016/j.applthermaleng.2017.10.019.

[10] Amiri Rad E, Mohammadi S. Energetic and exergetic optimized Rankine cycle for waste heat recovery in a cement factory. Appl Therm Eng 2018;132:410–22. https://doi.org/10.1016/j.applthermaleng.2017.12.076.

[11] Al-Sulaiman FA, Dincer I, Hamdullahpur F. Thermoeconomic optimization of three trigeneration systems using organic Rankine cycles: Part II - Applications. Energy Convers Manag 2013;69:209–16. https://doi.org/10.1016/j.enconman.2012.12.032.

[12] Puig-Arnavat M, Bruno JC, Coronas A. Modeling of trigeneration configurations based on biomass gasification and comparison of performance. Appl Energy 2014;114:845–56. https://doi.org/10.1016/j.apenergy.2013.09.013.

[13] Liu M, Shi Y, Fang F. Combined cooling, heating and power systems: A survey. Renew Sustain Energy Rev 2014;35:1–22. https://doi.org/10.1016/j.rser.2014.03.054.

[14] Wang Y, Shi Y, Ni M, Cai N. A micro tri-generation system based on direct flame fuel cells for residential applications. Int. J. Hydrogen Energy, vol. 39, 2014, p. 5996–6005. https://doi.org/10.1016/j.ijhydene.2014.01.183.

[15] Boyaghchi FA, Heidarnejad P. Thermodynamic analysis and optimisation of a solar combined cooling, heating and power system for a domestic application. Int J Exergy 2015;16:139. https://doi.org/10.1504/ijex.2015.068216.

[16] Bellos E, Tzivanidis C. Investigation of a hybrid ORC driven by waste heat and solar energy. Energy Convers Manag 2018;156:427–39. https://doi.org/10.1016/j.enconman.2017.11.058.

[17] Garg P, Orosz MS. Economic optimization of Organic Rankine cycle with pure fluids and mixtures for waste heat and solar applications using particle swarm optimization method. Energy Convers Manag 2018;165:649–68. https://doi.org/10.1016/j.enconman.2018.03.086.

[18] khanmohammadi S, Saadat-Targhi M. Performance enhancement of an integrated system with solar flat plate collector for hydrogen production using waste heat recovery. Energy 2019;171:1066–76. https://doi.org/10.1016/j.energy.2019.01.096.

[19] Khankari G, Karmakar S. Power generation from fluegas waste heat in a 500 MWe subcritical coal-fired thermal power plant using solar assisted Kalina Cycle System 11. Appl Therm Eng 2018;138:235–45. https://doi.org/10.1016/j.applthermaleng.2018.03.096.

[20] Júnior EPB, Arrieta MDP, Arrieta FRP, Silva CHF. Assessment of a Kalina cycle for waste heat recovery in the cement industry. Appl Therm Eng 2019;147:421–37. https://doi.org/10.1016/j.applthermaleng.2018.10.088.

[21] Ghasemi A, Heidarnejad P, Noorpoor A. A novel solar-biomass based multi-generation energy system including water desalination and liquefaction of natural gas system: Thermodynamic and thermoeconomic optimization. J Clean Prod 2018;196:424–37. https://doi.org/10.1016/j.jclepro.2018.05.160.

[22] Mostafavi Sani M, Noorpoor A, Shafie-Pour Motlagh M. Optimal model development of energy hub to supply water, heating and electrical demands of a cement factory. Energy 2019;177:574–92. https://doi.org/10.1016/j.energy.2019.03.043.

[23] Chakyrova D. Thermoeconomic Analysis of Biogas Engines Powered Cogeneration System. J Therm Eng 2019;5:93–107. https://doi.org/10.18186/thermal.532210.

[24] Keshtkar MM. Multi-Objective Optimization of a R744/R134a Cascade Refrigeration System: Exergetic, Economic, Environmental, and Sensitive Analysis (3Es). J Therm Eng 2019:237–50. https://doi.org/10.18186/thermal.581750.

[25] Ahmadi MH. Thermo-Environmental Analysis and Multi-Objective Optimization of Performance of Ericsson Engine Implementing an Evolutionary Algorithm. J Therm Eng 2019:319–40. https://doi.org/10.18186/thermal.582010.

[26] Jordán PS, Javier Eduardo AM, Zdzislaw MC, Alan Martín ZG, Liborio HP, Jesús Antonio FZ, et al. Techno-economic analysis of solar-assisted post-combustion carbon capture to a pilot cogeneration system in Mexico. Energy 2019;167:1107–19. https://doi.org/10.1016/j.energy.2018.11.010.

[27] Tregambi C, Salatino P, Solimene R, Montagnaro F. An experimental characterization of Calcium Looping integrated with concentrated solar power. Chem Eng J 2018;331:794–802. https://doi.org/10.1016/j.cej.2017.08.068.

[28] Almahdi M, Dincer I, Rosen MA. Analysis and assessment of methanol production by integration of carbon capture and photocatalytic hydrogen production. Int J Greenh Gas Control 2016;51:56–70. https://doi.org/10.1016/j.ijggc.2016.04.015.

[29] Novotny V, Vitvarova M, Kolovratnik M, Hrdina Z. Minimizing the Energy and Economic Penalty of CCS Power Plants Through Waste Heat Recovery Systems. Energy Procedia 2017;108:10–7. https://doi.org/10.1016/j.egypro.2016.12.184.

[30] Jakobsen J, Roussanaly S, Anantharaman R. A techno-economic case study of CO_2 capture, transport and storage chain from a cement plant in Norway. J Clean Prod 2017;144:523–39. https://doi.org/10.1016/j.jclepro.2016.12.120.

[31] Al-Sulaiman FA, Dincer I, Hamdullahpur F. Exergy modeling of a new solar driven trigeneration system. Sol Energy 2011;85:2228–43. https://doi.org/10.1016/j.solener.2011.06.009.

[32] Kalogirou SA. Summary for Policymakers. vol. 53. 2013. https://doi.org/10.1017/CBO9781107415324.004.

[33] Cengel YA, Boles MA. Summary for Policymakers. vol. 80. 2013. https://doi.org/10.1017/CBO9781107415324.004.

[34] Goswami DY. The CRC Handbook of Thermal Engineering. CRC Press; 2013.

[35] Petela R. Exergy of undiluted thermal radiation. Sol Energy 2003;74:469–88. https://doi.org/10.1016/S0038-092X(03)00226-3.

[36] Zamfirescu C, Dincer I. How much exergy one can obtain from incident solar radiation? J Appl Phys 2009;105:044911. https://doi.org/10.1063/1.3081637.

[37] Welcome | F-Chart Software : Engineering Software n.d.